

Reduction and fixation of Cr(VI) by *Aspergillus niger* along with bentonite-sodium alginate beads

Yinhuang Li, Ruixia Hao*, Bing Shan, Jiani Li, Yubo Ye, Junman Zhang, Anhuai Lu

The Key Laboratory of Orogenic Belts and Crustal Evolution, School of Earth and Space Sciences, Peking University, No. 5, Yiheyuan Road, Haidian District, Beijing 100871, China, emails: rxhao@pku.edu.cn (R. Hao), 1770241499@qq.com (Y. Li), shanbing@stu.pku.edu.cn (B. Shan), 2524776884@qq.com (J. Li), 2101110637@stu.pku.edu.cn (Y. Ye), pkuzjm@pku.edu.cn (J. Zhang), ahlu@pku.edu.cn (A. Lu)

Received 4 June 2022; Accepted 21 September 2022

ABSTRACT

Previous researches had demonstrated that microorganisms were able to reduce Cr(VI), which has been always regarded as a threat to human health. However, reduced Cr(III) exposed to natural environment is still possible to be re-oxidized to Cr(VI). In this present study, the system including *Aspergillus niger* and bentonite-sodium alginate beads (BSBs) was used to reduce and fix Cr(VI) from aqueous solution by batch mode. The *A. niger* and BSBs were characterized by spectrophotometry, inductively coupled plasma-optical emission spectroscopy (ICP-OES), scanning electron microscopy (SEM), transmission electron microscopy (TEM), energy-dispersive X-ray spectroscopy (EDS) and X-ray synchrotron radiation technology. Multiple mechanisms such as interlayer cation-exchange and bioremediation involved in Cr(VI) removal process. The results of spectrophotometry and TEM-EDS revealed the removal of Cr(VI) by *A. niger* through bioremediation. Also, the interlayer cation-exchange between Cr(III) and BSBs was revealed by ICP-OES, SEM-EDS and X-ray synchrotron radiation technology analysis. Experimental data showed that *A. niger* cultured in the system could reduce Cr(VI) nearly 100% while cell did not form intracellular Cr-containing minerals with trace amount of Cr in cell, and approximately 0.2 mg·L⁻¹ Cr(III) was fixed per gram of BSBs. This research provided a promising application of BSBs-*A. niger* system in Cr(VI) remediation where *A. niger* was capable of reducing Cr(VI) to Cr(III), and then Cr(III) could be immobilized through inter-layer cation-exchange by BSBs.

Keywords: Bioremediation; Chromium; Interlayer cation-exchange; Clay mineral; *Aspergillus niger*

1. Introduction

Cr(VI) discharged by anthropogenic activities like leather tanning, electroplating, and anodizing baths, has attracted global concerns about its harmful impacts on human health [1–3]. For example, Cr(VI) has various routes of exposure like dermal absorption, ingestion and inhalation, which causes skin ulceration and increases the risk of lung cancer in more severe cases [4]. Cr(VI) has more pathogenicity, mobility, and bioavailability than Cr(III) which means Cr(VI)

pollution is a complicated issue for human [5,6]. Accordingly, Cr(VI) has been categorized in class A human carcinogen by US Environmental Protection Agency (USEPA), and its maximum contaminant level is stringently constricted in 0.05 mg·L⁻¹ [7,8]. Remediation of Cr(VI) contamination is an imperative requirement for humans.

At present, traditional methods of Cr(VI) remediation include physical and chemical approaches, which are divided in adsorption, membrane filtration, ion exchange, and electrochemical treatment and so on by mechanisms

* Corresponding author.

[1,9,10]. These approaches have several drawbacks such as high-cost, high technology requirement and production of chemical sludge [11]. Consequently, microbial remediation gradually gained preference as an alternative to traditional physical and chemical methods, because it needs less expense and exerts less influence on environment [12–21].

Besides microorganisms, clay minerals like hydrotalcite [21], montmorillonite [23,24], zeolite [25], and bentonite [26–28] are also utilized by researchers to remediate metal pollution through cation interlayer exchange. However, the agglomeration and precipitation of clay mineral particles leads to deterioration of efficiency of metal contamination removal [29]. In order to eliminate this situation, researchers combine coagulant like sodium alginate with adsorbents to stabilize adsorbents. Sodium alginate imposes no direct influence on the removal of Cr(VI), because it couldn't remove Cr(VI) separately, and it could improve the efficiency of adsorbents through preventing from their aggregation [29–31].

This study investigated the Cr(VI) remediation by *Aspergillus niger* which is resistant to Cr [32], with beads consist of calcium bentonite and sodium alginate which could stabilize bentonite and prevent from aggregation of bentonite. Proportion of removed Cr(VI) was measured at different initial Cr concentrations, and the mechanism of Cr(VI) removal by *A. niger* with beads was revealed by inductively coupled plasma-optical emission spectroscopy (ICP-OES), scanning electron microscopy (SEM), transmission electron microscopy (TEM), energy-dispersive X-ray spectroscopy (EDS) and X-ray synchrotron radiation technology. This finding may provide a novel method for promoting efficiency of Cr(VI) remediation.

2. Materials and methods

2.1. *Aspergillus niger*, culture and bentonite-sodium alginate beads

A. niger used in experiments was preserved in the Microbial Geochemical Laboratory of Peking University [33], whose Cr(VI) tolerance reached up to 100 mg·L⁻¹. The culture medium (per L) contained NaCl 2 g, NaNO₃ 0.5 g, MgSO₄·7H₂O 5 mg, NH₄Cl 0.1 g, yeast extract 0.5 g, beef extract 1 g, tryptone 3 g, and glucose 3 g [33].

The production method of bentonite-sodium alginate beads (BSBs) is shown in Fig. 1 and as follows: 3 g

bentonite and 2 g sodium alginate were completely mixed in 100 mL deionized water. And then, we added the mixture into high-pressure steam sterilization pot heated to 120°C for 1 h. As soon as the temperature dropped to 70°C, we took it out of pot then immediately injected the mixture evenly into sterile 1% CaCl₂ solution by a sterile syringe. The homogeneous BSBs (beads with diameter 2 mm) were obtained after cooling in 1% CaCl₂ solution for 12 h.

2.2. Influence of different initial Cr(VI) concentrations on Cr(VI) removal efficiency

A. niger was pre-cultured in medium for 48 h in LRH-150 incubator (Shanghai Qixin Scientific Instrument Co., Ltd., Shanghai, China) at 30°C ± 0.5°C, 150 rpm. After incubation, 1 mL inoculum and 10 g BSBs were added into new mediums respectively (Fig. 1) with a series of Cr(VI) concentrations (10, 30 and 50 mg·L⁻¹, initial pH 5.7), with a medium containing 50 mg·L⁻¹ Cr(VI) without *A. niger* as a control group. All the mediums were then incubated at 30°C ± 0.5°C, 150 rpm for 18 d. Proportion of removed Cr(VI) (*P*) was calculated by the equation:

$$P_{\text{Cr(VI)}}(\%) = \frac{(C_{\text{Cr(VI)}}^i - C_{\text{Cr(VI)}}^f)}{C_{\text{Cr(VI)}}^i} \times 100\% \quad (1)$$

where $C_{\text{Cr(VI)}}^i$ means initial concentration of Cr(VI) (mg·L⁻¹) and $C_{\text{Cr(VI)}}^f$ means final concentration of Cr(VI) (mg·L⁻¹) [32].

Total Cr (Cr(III) and Cr(VI)) and Cr(VI) concentrations were measured every day. Cr(III) was expressed as the value of total Cr minus Cr(VI) contents. Total Cr was measured by inductively coupled plasma-optical emission spectroscopy (ICP-OES; Spectro Blue SOP). And Cr(VI) was determined by sensitive and selective reaction between Cr(VI) and diphenylcarbazide (DPCI) through spectrophotometric methods (Thermo Evolution 220) at 540 nm [34,35].

2.3. Influence of different weight of BSBs on amount of fixed total Cr

In order to investigate the influence of the weight of BSBs on amount of fixed total Cr, 5 or 20 g BSBs and 1 mL inoculum were added into new mediums respectively with a same series of Cr(VI) concentrations. All the

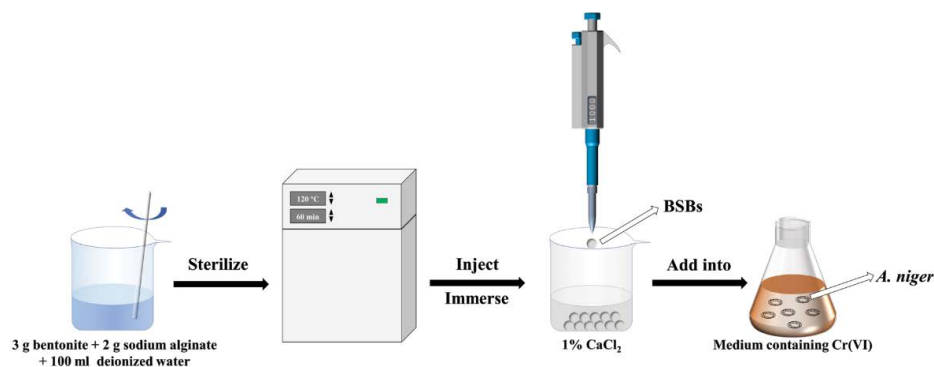


Fig. 1. Schematic diagram of the synthesis mechanism of BSBs-*A. niger* system.

mediums were then incubated at $30^{\circ}\text{C} \pm 0.5^{\circ}\text{C}$, 150 rpm for 18 d. Proportion of remained total Cr (R) was calculated by the equation:

$$R_{\text{Cr}}(\%) = \frac{C_{\text{Cr}}^f}{C_{\text{Cr}}^i} \times 100\% \quad (2)$$

where C_{Cr}^i means initial concentration of total Cr ($\text{mg}\cdot\text{L}^{-1}$), C_{Cr}^f means final concentration of total Cr ($\text{mg}\cdot\text{L}^{-1}$). Removed total Cr concentration per gram of BSBs (S) was calculated by the equation:

$$S_{\text{Cr}}(\text{mg}(\text{L}\cdot\text{g})^{-1}) = \frac{C_{\text{Cr}}^i - C_{\text{Cr}}^f}{M_{\text{BSBs}}} \quad (3)$$

where C_{Cr}^i means initial concentration of total Cr ($\text{mg}\cdot\text{L}^{-1}$), C_{Cr}^f means final concentration of total Cr ($\text{mg}\cdot\text{L}^{-1}$), M_{BSBs} means weight of BSBs added into medium (g).

2.4. Morphological study of minerals and fungus

Morphology and elemental composition of *A. niger* participating in removing Cr(VI) process was examined by TEM and EDS. Fungal strain was cultivated in mediums with BSBs containing a series of initial Cr(VI) concentration gradient (10, 30 and $50 \text{ mg}\cdot\text{L}^{-1}$) at 30°C . After 18 d, *A. niger* was extracted as fungal pellets and rinsed by 0.1 M phosphate buffer (pH 7) three times (20 min each time), and then transferred into 2.5% glutaraldehyde which first kept at room temperature for 2 h then kept at 4°C for 12 h. Subsequently, we used 1% osmic acid to fix fungal pellets at 1°C for 1 h and then washed them with 0.1 M phosphate buffer (pH 7) for 30 min. The fungal cells were dehydrated by acetone with a series of concentration gradient (30%, 50%, 70%, 85%, 95%, and 100% concentrations), kept in each concentration for 7 min, and treated twice with 100% acetone. Next, the fungal cells were treated by resin–acetone mixtures with a series of volume fraction (V:V = 3:1, 1:1, and 1:3) for different time (0.5, 1.0, and 1.5 h, respectively) and then kept in pure resin overnight; after this, the samples were treated with fresh resin for 2 h. We embedded the samples by incubation of them in new tubes at 60°C for 24 h; then, the samples were sectioned by an ultrathin microtome to obtain 100 nm sections and fixed on a copper network coated with a micro-sand carbon film. The samples were observed under a field emission TEM (JEM-2100F) with a high voltage of 200 kV.

Morphology and elemental composition of BSBs before and after Cr(VI) removal process was examined by SEM and EDS. After 18 d incubation, BSBs added in culture medium incubating *A. niger* with initial $50 \text{ mg}\cdot\text{L}^{-1}$ Cr(VI) were extracted, and BSBs added in initial $50 \text{ mg}\cdot\text{L}^{-1}$ Cr(VI) medium without *A. niger* used as a control. Next, the extracted BSBs were rinsed by ethyl alcohol for 10 min in order to remove irrelevant organic metabolites. After this process, BSBs were washed by 0.05 M phosphate buffer (pH 7) for 5 min. And then, BSBs were fixed on conductive adhesive tape and stored in refrigerator at 4°C for 12 h. A field-emission environmental SEM (ESEM) (FEI Quanta

200 FEG) and an auxiliary EDS (Oxford) at 15 kV and 120 Pa were used to observe BSBs in experiments.

2.5. Investigation of interlayer ion exchange process in BSBs

The X-ray diffraction (XRD) data of BSBs were collected at BL17B1 beamline in Shanghai Synchrotron Radiation Facility (SSRF) at 16000 eV. 2D distribution of relationship between intensity and 2θ was obtained by software fit2d (v12.077). And then the data were analyzed by software highplus to identify whether crystalline interplanar spacing of BSBs participating in Cr removal process, which indicated the phenomenon of interlayer ion exchange.

3. Results

3.1. Influence of different initial Cr(VI) concentrations on Cr(VI) removal efficiency

Compared with control group, Fig. 2 shows culture mediums incubating *A. niger* all had ability to remove nearly 100% Cr(VI), while the removal rate declined along with the initial Cr(VI) concentration increased. When the initial Cr(VI) concentration was $10 \text{ mg}\cdot\text{L}^{-1}$, *A. niger* reduced all Cr(VI) to Cr(III) in 12 d, while the initial Cr(VI) concentrations were 30 and $50 \text{ mg}\cdot\text{L}^{-1}$, *A. niger* took 18 d to remove all Cr(VI) from the culture mediums.

3.2. Influence of different weight of BSBs on amount of fixed total Cr

The changes in concentration of total Cr in mediums with different amount of BSBs at a series of initial Cr concentrations along with incubation time are shown in Fig. 3. Total Cr concentration in mediums reduced by 1.3, 2 and $3.4 \text{ mg}\cdot\text{L}^{-1}$ with 5, 10 and 20 g BSBs respectively at initial Cr concentration $10 \text{ mg}\cdot\text{L}^{-1}$ (Fig. 3A); total Cr concentration in mediums reduced by 1.4, 2.4 and $4.5 \text{ mg}\cdot\text{L}^{-1}$ with 5, 10 and 20 g BSBs respectively at initial Cr concentration $30 \text{ mg}\cdot\text{L}^{-1}$ (Fig. 3B); total Cr concentration in mediums

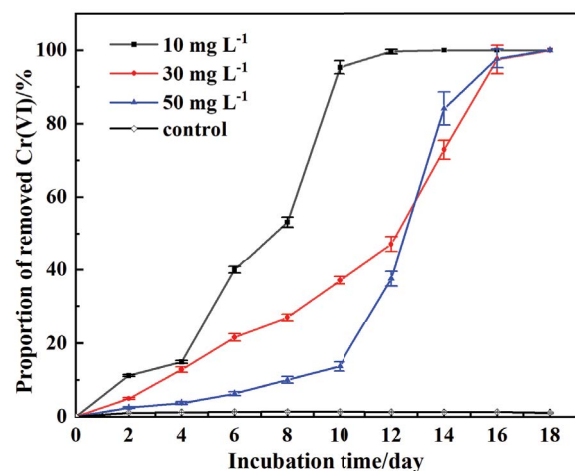


Fig. 2. Proportion of removed Cr(VI) along with incubation time under different initial Cr(VI) concentrations (10, 30 and $50 \text{ mg}\cdot\text{L}^{-1}$) with *A. niger* and BSBs.

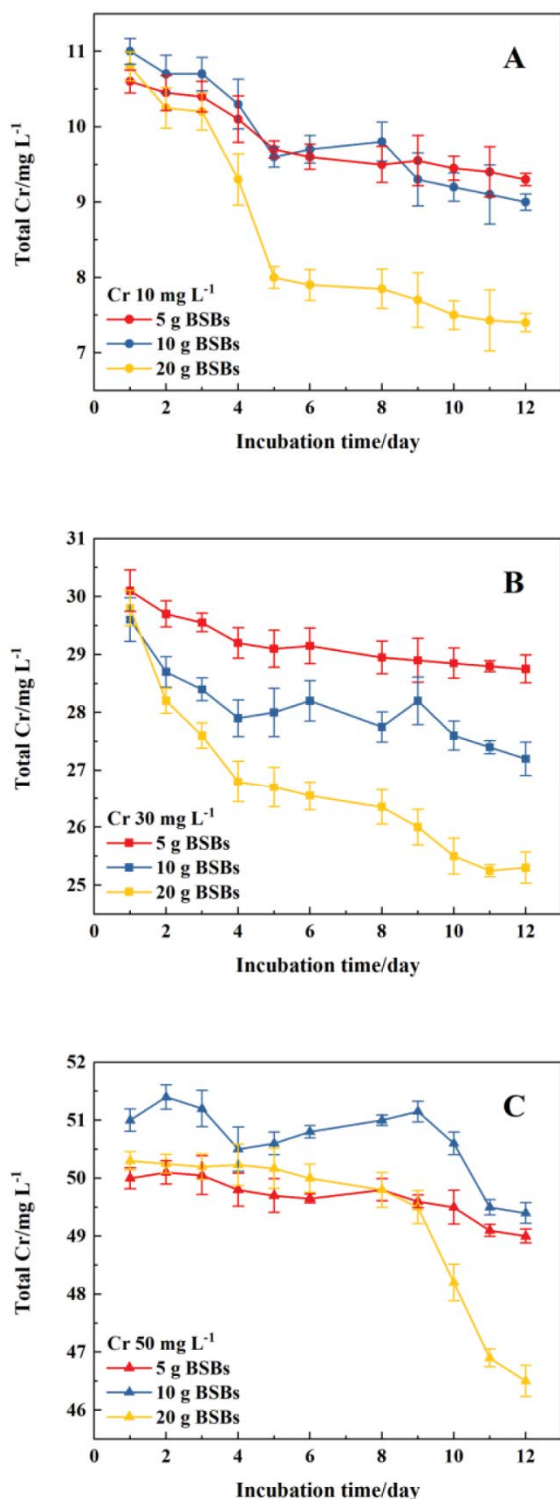


Fig. 3. Changes of total Cr concentration along with incubation time in medium containing different weight of BSBs (5, 10 and 20 g) with 10 (A), 30 (B) and 50 (C) mg·L⁻¹ initial Cr, respectively.

reduced by 1.0, 1.6 and 3.8 mg·L⁻¹ with 5, 10 and 20 g BSBs respectively at initial Cr concentration 50 mg·L⁻¹ (Fig. 3C). The results showed that at the same initial Cr concentration, the changes of total Cr concentration increased with

the increase of BSBs. But the changes of total Cr concentration in mediums at different initial Cr concentration with the same amount of BSBs were similar. In all experimental groups, total Cr concentration in mediums with 5 g BSBs reduced by approximate 1.0–1.4 mg·L⁻¹, total Cr concentration in mediums with 10 g BSBs reduced by approximate 1.6–2.4 mg·L⁻¹; total Cr concentration in mediums with 20 g BSBs reduced by approximate 3.4–4.5 mg·L⁻¹ (Fig. 3).

Comparing remaining total Cr concentration with initial total Cr concentration, we obtained the percentage of remaining total Cr. Fig. 4 presents proportions of remaining total Cr with initial total Cr in different experimental groups with different amount of BSBs at a series of initial Cr concentrations. In experimental groups with 5 g BSBs, 87.74% ($\pm 0.77\%$), 95.52% ($\pm 0.80\%$) and 98.00% ($\pm 0.24\%$) of total Cr remained in mediums at initial total Cr concentrations 10, 30 and 50 mg·L⁻¹, respectively (Fig. 4A); in experimental groups with 10 g BSBs, 81.81% ($\pm 0.352\%$), 91.89% ($\pm 1.279\%$) and 96.86% ($\pm 2.471\%$) of total Cr remained in mediums with initial total Cr concentrations 10, 30 and 50 mg·L⁻¹, respectively (Fig. 4B); in experimental groups with 20 g BSBs, 68.51% ($\pm 1.13\%$), 84.90% ($\pm 0.90\%$) and 92.45% ($\pm 0.54\%$) of total Cr remained in mediums at initial total Cr concentrations 10, 30 and 50 mg·L⁻¹, respectively (Fig. 4C). These results suggested remaining total Cr decrease with the increase of BSBs. But the removed total Cr concentration per gram of BSBs in all experimental groups was similar (approximately 0.2 mg·(L·g)⁻¹). In experimental groups with 5, 10 and 20 g BSBs, removed total Cr concentration per gram of BSBs was 0.2–0.27, 0.19–0.24 and 0.17–0.23 mg·(L·g)⁻¹, respectively (Fig. 4A–C).

3.3. Morphology of BSBs investigated by SEM

SEM revealed morphological difference of BSBs exposed to 50 mg·L⁻¹ Cr(VI) before and after incubation, and elemental composition of their surface was obtained by EDS. Morphology of BSBs with *A. niger* in Fig. 5D presents smooth surface, Fig. 5E and F show mass fraction of Cr at different spots in Fig. 5D, which were 2.6% and 4.0%, respectively. However, BSBs in the control group had opposite characterization (Fig. 5A) that its appearance transformed into roughness. Besides, Cr mass fraction of selected spots (Fig. 5B and C) were higher than spots in Fig. 5D, which reached up to 8.5%. EDS data confirmed that Cr was present at BSBs in a specific form, and SEM images suggested that Cr(VI) indeed changed morphology of BSBs which might be concerned with the way BSBs immobilizing Cr(VI).

3.4. Insight of bentonite interlayer spacing provided by X-ray synchrotron radiation

XRD data collected at BL17B1 beamline in SSRF performed with synchrotron radiation ($\lambda = 0.07749$ nm). BSBs containing sodium alginate and bentonite, while bentonite was compound, mainly composed of montmorillonite. Because of their complicated composition, Fig. 6A data show characterization of various material, we speculated that it was caused by sodium alginate, bentonite and CaCl₂ solution as raw materials of BSBs. Therefore, besides the peaks only representing d_{001} lattice plane of montmorillonite

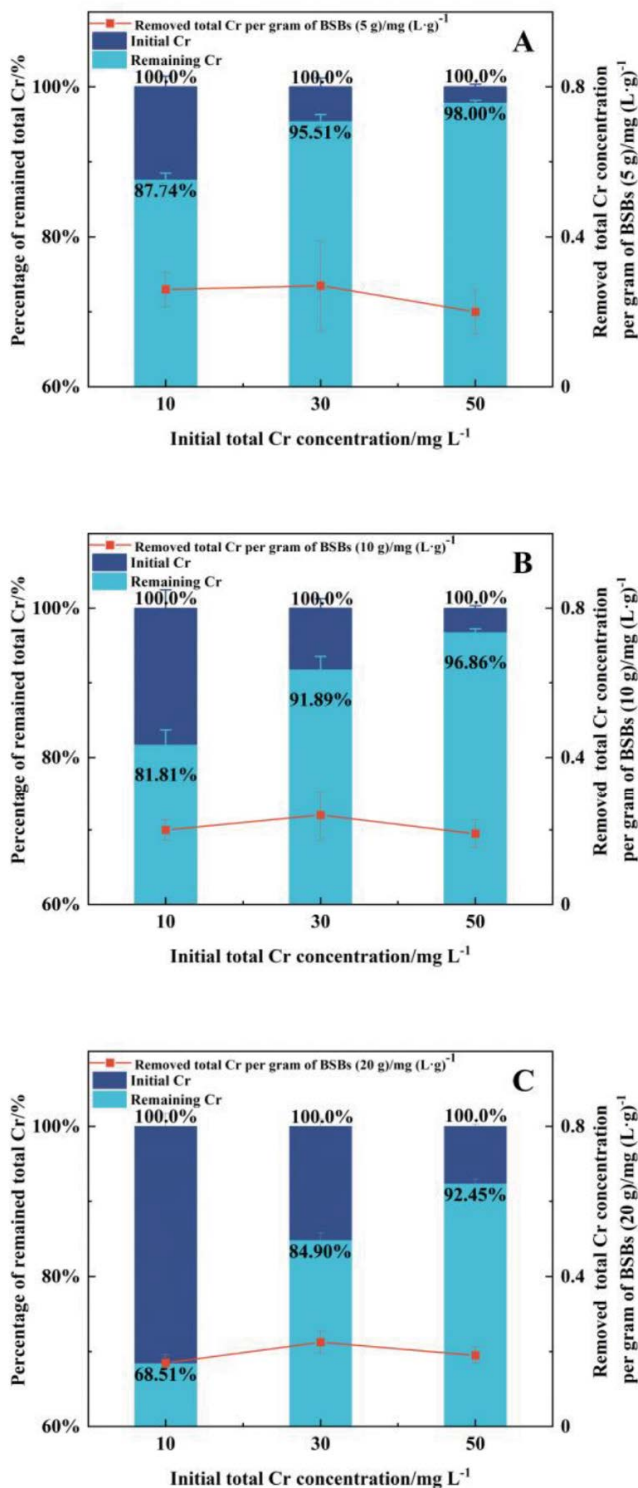


Fig. 4. Percentage of remained total Cr concentration after incubation compared to initial total Cr concentration with a series of initial Cr concentrations (10, 30 and 50 mg·L⁻¹) in medium containing 5 (A), 10 (B) and 20 (C) g BSBs. Red square indicates the removed total Cr concentration per gram of BSBs.

which provided an insight into changes of interlayer spacing, there are other characteristic peaks with higher intensity. Montmorillonite had characteristic feature at $d_{001} = 1.429$ nm [36], and d -spacing and X-ray wavelength follows equation:

$$2d \sin \theta = \lambda \quad (4)$$

where d refers to d -spacing (nm), θ is angle of incidence, and λ is wavelength of X-ray radiation (nm).

Fig. 6B shows montmorillonite d_{001} characteristic peaks at $2\theta = 3.1365^\circ$, 2.7337° and 2.5728° in the condition of (i) BSBs, (ii) BSBs with $50 \text{ mg}\cdot\text{L}^{-1}$ Cr(VI), (iii) BSBs with $50 \text{ mg}\cdot\text{L}^{-1}$ Cr(VI) and *A. niger*, respectively. Utilizing formula above, corresponding d -spacings were 1.415739, 1.624292 and 1.725845 nm in turn. We found that the d -spacings (from 1.415739 to 1.725845 nm) of montmorillonite increased after adding Cr(VI) and *A. niger*.

3.5. Intracellular structure and Cr distribution of *A. niger*

A. niger incubated in mediums with 10, 30 and $50 \text{ mg}\cdot\text{L}^{-1}$ Cr(VI) was analyzed by TEM and EDS (Fig. 7), intending to provide insight into the distribution of Cr in fungal cells. According to TEM micrographs, no obvious mineral crystal particles were captured in cell (Fig. 7A, C and E). Besides, EDS mapping scan data demonstrated that Cr content of total scanning area was nearly 0.01% in all samples ($10, 30$ and $50 \text{ mg}\cdot\text{L}^{-1}$) (Fig. 7B, D and E), indicating in these experiments, a small amount of Cr was transferred into fungal cells.

4. Discussion

Cr(VI) is harmful to human, and this BSBs–*A. niger* combined method might offer a novel and complete approach for Cr remediation, but insight into the Cr remediation mechanism needs to be provided. Cr(VI) species and Cr(III) species existed in medium containing both *A. niger* and Cr(VI) because of *A. niger* reduction process [32], while BSBs themselves were not able to reduce Cr(VI) so that mainly Cr(VI) species existed in medium containing BSBs and Cr(VI). Bentonite entrapped in BSBs was often used as adsorbent for Cr(VI) in previous study [37,38]. In order to understand how BSBs and *A. niger* interacted with Cr in the mixed culture of BSBs, *A. niger* and Cr(VI), this study analyzed the variation of total Cr and Cr(VI) concentrations in medium and observed the morphology and elemental distribution of BSBs and *A. niger*.

4.1. Removal of Cr(VI) and change of total Cr concentration

Fig. 2 demonstrates that BSBs–*A. niger* system removed nearly 100% Cr(VI) in every experimental group, indicating almost all Cr(VI) was reduced and existed in the form of Cr(III). We considered that *A. niger* played a major role in this reducing process, which was similar with previous researches [39–44]. Figs. 3 and 4 show that total Cr concentration decreased which was measured by ICP-OES, and there were two possible processes leading to the decrease. The first process might be the interlayer cation-exchange, which occurred between clay minerals and metal ions. Previous researches revealed that clay minerals were mostly combination of octahedral and tetrahedral sheets. In these structures, cations with comparable radius could substitute original cations, resulting in residual negative charges. And these negative charges would be neutralized by adsorption of alkali earth cations. After neutralization, these alkali earth cations had the potential to be replaced by other cations, including heavy metal ions [45]. Another presumable

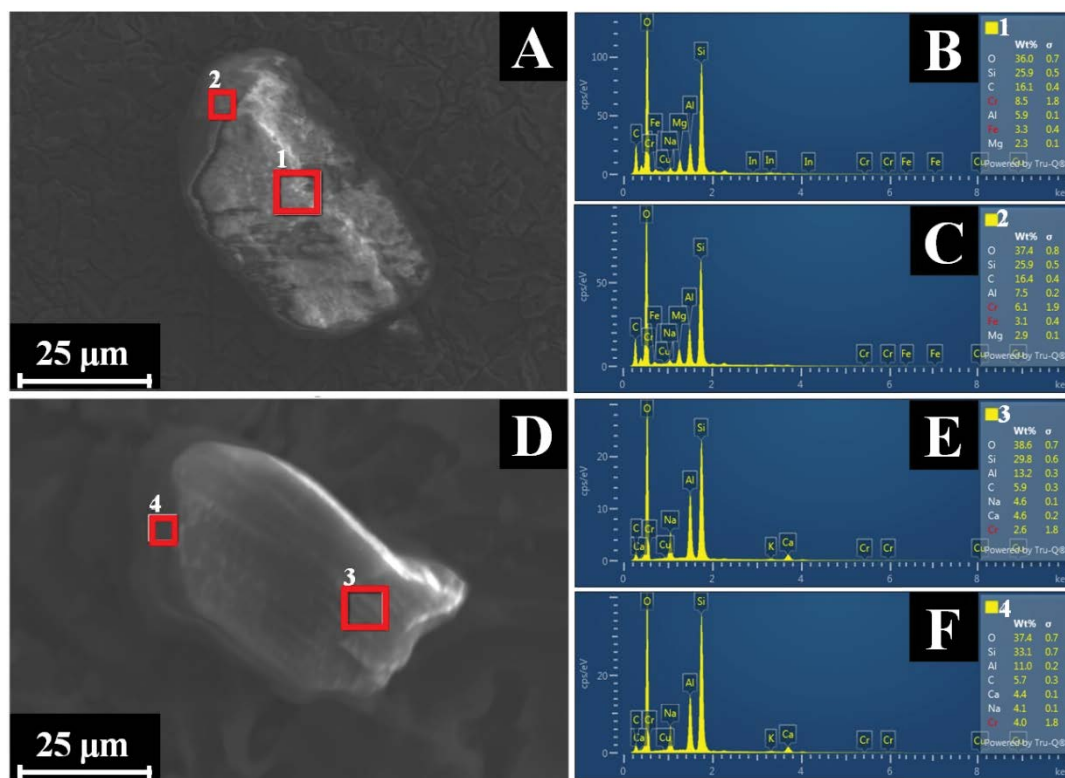


Fig. 5. SEM images of BSBs placed in medium containing $50 \text{ mg}\cdot\text{L}^{-1}$ Cr without (A) and with (D) *A. niger*; elemental mass fraction of them collected by EDS next to corresponding images (B and C from areas marked 1 and 2 in A, E and F from areas marked 3 and 4 in D). The samples were collected at day 18.

process contributing to the total Cr content decrease was biological fixation. Plenty of examples about biomineralization were documented [46–48], but *A. niger* had not been found to form stable Cr(III) minerals. Metal ions could enter into microorganism by ion channels, gathering in cell which might cause decrease of Cr concentration in aqueous solution. There was no exclusive ion channel dedicated to Cr, though certain microorganisms had the ability to allow Cr to enter into cells through other iso-valent ion channels and reduced it under certain circumstances [49]. To determine which process played a major role, this study observed the morphology and elemental distribution of BSBs and *A. niger*, respectively.

4.2. Fixation of Cr by BSBs

Fig. 5 shows SEM pictures comparing morphology of BSBs placed in medium containing Cr(VI) with and without *A. niger*. Fig. 5A and D show the difference of surface smoothness between BSBs exposed to microbial activity or not which clearly indicated the distinction BSBs treated Cr(VI) and Cr(III) species. When BSBs processed Cr(VI) without *A. niger*, BSBs showed rough surface (Fig. 5A). The result corresponded with the property of clay mineral whose surficial functional groups were capable of combining with Cr(VI) [50]. In the absence of *A. niger*, system lacked the ability to reduce Cr(VI) to Cr(III), and clay minerals were difficult to exchange with dichromate anions containing

Cr(VI). Under continuous exposure to the BSBs surface without interference, a batch of Cr(VI) ions were captured by surface adsorption, which transformed BSBs' surface morphology. Contrary to BSBs without *A. niger*, BSBs with *A. niger* displayed a smooth surface (Fig. 5A and D). Because of the existence of *A. niger*, its growth and metabolism continuously influenced the system, which made the surface adsorption of BSBs difficult (lack of an undisturbed environment). Microbes removed Cr(VI) in various mechanisms, and various cell fractions owned the ability to reduce the Cr(VI), including cell free extracts (CFE), cell secretions, and cell debris [39,51–53]. The process of cell reduction of Cr(VI) would compete with surface adsorption for Cr(VI), which suppressed the surface adsorption, maintaining the smoothness of BSBs surface. Even if surface adsorption occurred, microbes attached to the surface of BSBs still snatched back the Cr(VI). Therefore, Cr(VI) preferentially reacted with *A. niger* and was reduced to Cr(III), then partial Cr(III) in the medium would enter into the clay mineral interlayer, which was unlike Cr(VI) enriched on the surface of BSBs without the influence of *A. niger*. This mechanism explained why Cr mass fraction on surface of BSBs only exposed to Cr(VI) was significantly higher than it on surface of BSBs exposed to Cr(VI) and *A. niger* (Fig. 5B, C, E and F).

X-ray synchrotron radiation provided more reliable evidence about Cr(III) entering into interlayer structure of BSBs. BSBs were composed of clay minerals mainly containing bentonite and sodium alginate, and bentonite was

able to interact with Cr(III) [27,38,54]. Previous studies showed that the entry of Cr(III) into interlayer of montmorillonite could lead to the expansion of d_{001} [55]. Therefore, we focused on the change of characteristic peak of d_{001} lattice plane in order to find evidence of Cr(III) entering into crystal lattice. Fig. 6 shows XRD data collected from BSBs which show montmorillonite d_{001} characteristic peaks at $2\theta = 3.1365^\circ$, 2.7337° and 2.5728° when BSBs were in mediums (i) without Cr(VI) and *A. niger*, (ii) with Cr(VI), and (iii) with Cr(VI) and *A. niger*, respectively. Bring these θ data into the formula $2d\sin\theta = \lambda$, d representing the d -spacing were 1.415739, 1.624292 and 1.725845 nm, respectively. It could be clearly seen that montmorillonite had increased from 1.415739 to 1.725845 nm after co-processing Cr(VI) with *A. niger*. The change in the thickness of the d_{001} was intuitive for the occurrence of interlayer cation-exchange.

4.3. Accumulation of Cr by *A. niger*

In addition to entering into the interlayer of BSBs, Cr might accumulate in *A. niger* cells. The intracellular structures of *A. niger* cells extracted from the mediums with the initial Cr(VI) concentrations of 10, 30, and 50 mg·L⁻¹ were clearly seen by TEM. No obvious mineral crystals appeared in the cells at different initial Cr(VI) concentrations (Fig. 7A, C and E). EDS mapping scan analyzed these *A. niger* cells, and trace amount of Cr was detected (Fig. 7B, D and F), where Cr weight percentage of these cells was less than 0.5%. The small amount of Cr in the cells was related to the reduction mechanism of *A. niger*. We speculated that the Cr(VI) reduction process required Cr(VI) to enter into cells and be reduced by reductase. Previous researches demonstrated that functional groups like amino and phosphoryl on cell wall interact with Cr(VI) ions which retained them on cell wall [32]. Subsequently partial Cr(VI) was transferred into cells via surface ion channels, which were most likely sulfate channel due to the similarity between dichromate and sulfate ions structures [56,57]. After entering into cells, on account of the widespread of

reductase in the cytoplasm, as soon as the Cr(VI) was transferred into the cells, it was exposed to a reducing environment and then was reduced to Cr(III). Finally, the Cr(III) was excreted from the cell through *ChrA* transmembrane protein (Gupta et al. [56]). This process could be considered as the detoxification mechanism of cells to prevent cells from being damaged by Cr(VI), and small amount of reduced Cr(III) ions had not been discharged from the cells were detected by EDS in this study.

EDS showed the amount of Cr accumulated in *A. niger* was too small, so it was the former process—interlayer cation-exchange playing a major role in the decrease of total Cr concentration. Total Cr concentration in mediums with 5, 10 and 20 g BSBs reduced by 1.0–1.4, 1.6–2.4 and 3.4–4.5 mg·L⁻¹, respectively (Fig. 3A–C). These results suggested the amount of removed total Cr in system was mainly influenced by the weight of BSBs, therefore in the experimental groups with same weight of BSBs, amount of removed Cr was similar, and in the experimental groups with same initial Cr concentration, amount of removed Cr increased with the increase of BSBs. It might result from that unit mass of BSBs added into each mediums have the same capacity of interlayer cation-exchange with Cr(III). Corresponding with Fig. 4, it presents similar removed total Cr concentration per gram of BSBs (approximately 0.2 mg·(L·g)⁻¹). Fig. 4 also shows the decrease of total Cr didn't reach up to 100%, while the amount of removed Cr(VI) was nearly 100% in every experimental group (Fig. 2), and it was also constricted by the interlayer cation-exchange process. Because unit mass of BSBs have the same capacity of interlayer cation-exchange with Cr(III), adding more BSBs could raise the percentage of removed Cr. Besides the amount of BSBs, various parameters could also influence the removal of Cr. Previous research revealed that interlayer cation-exchange proceeded slowly when changes in conditions such as temperature and pH would affect this process [45]. And in this experiment, system placed in normal temperature and pressure, the condition was more conducive to the growth of *A. niger*, causing bioremediation more obvious.

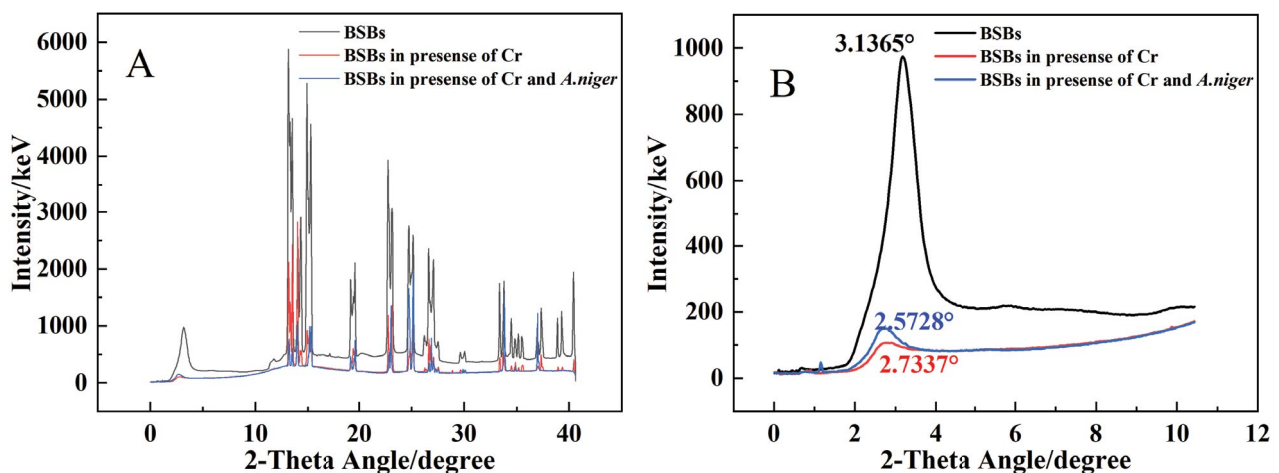


Fig. 6. (A) X-ray diffraction (XRD) of BSBs, BSBs in presence of 50 mg·L⁻¹ Cr and BSBs in presence of 50 mg·L⁻¹ Cr and *A. niger* and (B) enlarged particular filed of Fig. 6A ranging from 0° to 12° where 2θ angle of d_{001} characteristic peaks of montmorillonite are marked. The samples were collected at day 18.

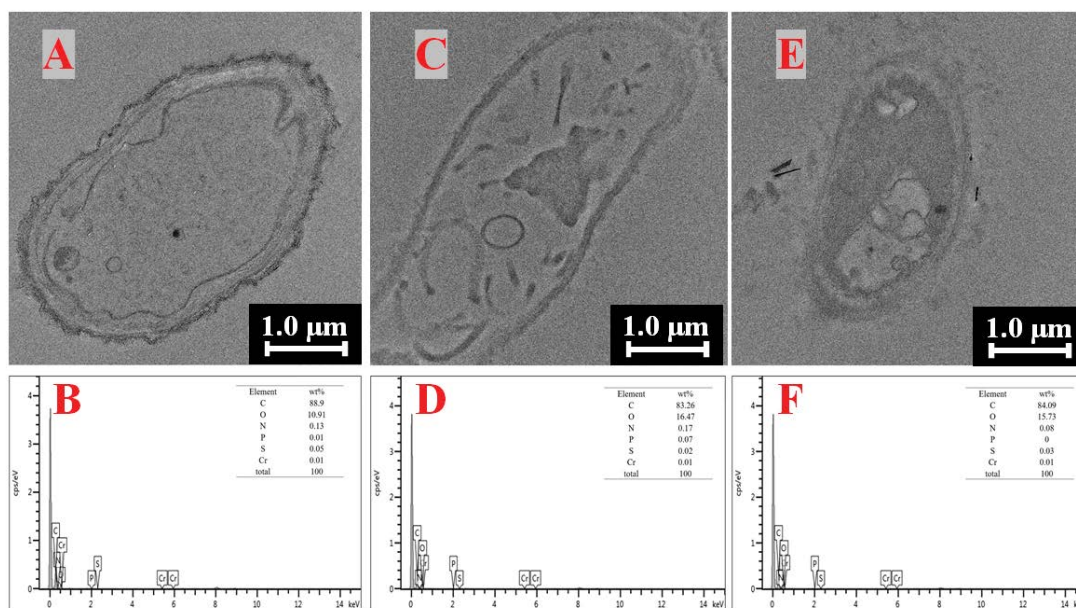


Fig. 7. TEM (above) images and EDS (below) of *A. niger* cultured in medium with 10 (A,B), 30 (C,D) and 50 (E,F) mg·L⁻¹ Cr(VI). The samples were collected at day 18.

5. Conclusions

This system contained *A. niger* and bentonite mainly removing Cr(VI) in a way of reducing it to Cr(III) by microorganisms. The whole system was capable of approximately reducing all Cr(VI) to Cr(III). Then overwhelming majority of reduced Cr(III) existed in the form of soluble ions in aqueous solution, and the residual small part of Cr(III) mainly existed in two forms. The first form was the Cr(III) participating in interlayer cation-exchange with BSBs, which could fix 0.2 mg·L⁻¹ Cr(III) per gram, and these Cr(III) resulted in bentonite d_{001} expanding. Another form was the Cr(III) accumulating in *A. niger*, and these Cr(III) originated from the entry of Cr(VI) via ion channels, then Cr(VI) was reduced to Cr(III) by intracellular reductase, finally a small amount of Cr(III) was immobilized in cells. Although not 100% Cr(III) was fixed in this experiment, the amount of removed Cr(III) could be increased by adding more BSBs, and the interlayer cation-exchange capacity of clay minerals for Cr(III) could be improved by approaches of clay mineral modification and changing the reaction conditions. These findings provided a new and promising method, which not only reduce Cr(VI) but also immobilize Cr(III), preventing it from being oxidized again to contaminate environment. We will shed light on the mechanism of microbial Cr(VI) remediation in the future research.

Funding

This work was supported by the National Natural Science Foundation of China under Grant 41672332; National Key Research and Development Project of China under Grant 2019YFC1805901; National Basic Research Program of China under Grant 2014CB846003.

Disclosure statement

The author report there are no competing interests to declare.

Acknowledgements

We are grateful grants from the National Natural Science Foundation of China (41672332), National Key Research and Development Project of China (2019YFC1805901) and National Basic Research Program of China (2014CB846003). We thank all the colleagues and students who make contribution in this research, and we also thank Jingnan Liang at Institute of Microbiology Chinese Academy of Sciences for her assistance in the preparation of TEM slice.

References

- [1] M. Owwad, M.K. Aroua, W.A.W. Daud, S. Baroutian, Removal of hexavalent chromium-contaminated water and wastewater: a review, *Water Air Soil Pollut.*, 200 (2009) 59–77.
- [2] Y. Li, Q. Zhou, B. Ren, J. Luo, J. Yuan, X. Ding, H. Bian, X. Yao, Trends and health risks of dissolved heavy metal pollution in global river and lake water from 1970 to 2017, *Rev. Environ. Contam. Toxicol.*, 251 (2020) 1–24.
- [3] D.J. Paustenbach, B.L. Finley, F.S. Mowat, B.D. Kerger, Human health risk and exposure assessment of chromium(VI) in tap water, *J. Toxicol. Environ. Health Part A*, 66 (2001) 1295–1339.
- [4] D.E. Kimbrough, Y. Cohen, A.M. Winer, L. Creelman, C. Mabuni, A critical assessment of chromium in the environment, *Crit. Rev. Env. Sci. Technol.*, 29 (1999) 1–46.
- [5] G. Choppala, N. Bolan, J.H. Park, Chapter Two – Chromium Contamination and Its Risk Management in Complex Environmental Settings, In: *Advances in Agronomy*, Vol. 120, 2013, pp. 129–172.
- [6] D.A. Eastmond, J.T. MacGregor, R.S. Slesinski, Trivalent chromium: assessing the genotoxic risk of an essential trace

- element and widely used human and animal nutritional supplement, *Crit. Rev. Toxicol.*, 38 (2008) 173–190.
- [7] D. Pradhan, L.B. Sukla, M. Sawyer, P.K.S.M. Rahman, Recent bioreduction of hexavalent chromium in wastewater treatment: a review, *J. Ind. Eng. Chem.*, 55 (2017) 1–20.
- [8] K. Zhu, Y. Duan, F. Wang, P. Gao, H. Jia, C. Ma, C. Wang, Silane-modified halloysite/Fe₃O₄ nanocomposites: simultaneous removal of Cr(VI) and Sb(V) and positive effects of Cr(VI) on Sb(V) adsorption, *Chem. Eng. J.*, 311 (2017) 236–246.
- [9] S. Rengaraj, K.H. Yeon, S.H. Moon, Removal of chromium from water and wastewater by ion exchange resins, *J. Hazard. Mater.*, 87 (2001) 273–287.
- [10] V.K. Gupta, S. Agarwal, T.A. Saleh, Chromium removal by combining the magnetic properties of iron oxide with adsorption properties of carbon nanotubes, *Water Res.*, 45 (2011) 2207–2212.
- [11] D. Mamais, C. Noutsopoulos, L. Kavallaris, E. Nyktari, A. Kaldis, E. Panousi, N. George, A. Kornilia, M. Nasioka, Biological groundwater treatment for chromium removal at low hexavalent chromium concentrations, *Chemosphere*, 152 (2016) 238–244.
- [12] Q. Zhou, Y. Liu, T. Li, H. Zhao, S.A. Daniel, W. Liu, O.K. Kurt, Cadmium adsorption to clay-microbe aggregates: implications for marine heavy metals cycling, *Geochim. Cosmochim. Acta*, 290 (2020) 124–136.
- [13] M. Narayani, K. Vidya Shetty, Chromium-resistant bacteria and their environmental condition for hexavalent chromium removal: a review, *Crit. Rev. Env. Sci. Technol.*, 43 (2013) 955–1009.
- [14] P.M. Fernández, S.C. Viñarta, A.R. Bernal, E.L. Cruz, L.I.C. Figueroa, Bioremediation strategies for chromium removal: current research, scale-up approach and future perspectives, *Chemosphere*, 208 (2018) 139–148.
- [15] R. Jobby, P. Jha, A.K. Yadav, N. Desai, Biosorption and biotransformation of hexavalent chromium [Cr(VI)]: a comprehensive review, *Chemosphere*, 207 (2018) 255–266.
- [16] F.J. Acevedo-Aguilar, A.E. Espino-Saldaña, I.L. Leon-Rodríguez, M.E. Rivera-Cano, M. Avila-Rodríguez, K. Wrobel, K. Wrobel, P. Lappe, M. Ulloa, J.F. Gutiérrez-Corona, Hexavalent chromium removal in vitro and from industrial wastes, using chromate-resistant strains of filamentous fungi indigenous to contaminated wastes, *Can. J. Microbiol.*, 52 (2006) 809–815.
- [17] R. Batool, K. Yrjala, S. Hasnain, Hexavalent chromium reduction by bacteria from tannery effluent, *J. Microbiol. Biotechnol.*, 22 (2012) 547–554.
- [18] A. Bingol, H. Uzun, Y.K. Bayhan, A. Karagunduz, A. Cakici, B. Keskinler, Removal of chromate anions from aqueous stream by a cationic surfactant-modified yeast, *Bioresour. Technol.*, 94 (2004) 245–249.
- [19] V. Mary Kensa, Bioremediation – an overview, *J. Ind. Pollut. Control*, 27 (2011) 161–168.
- [20] D. Onyancha, W. Mavura, J. Catherine Ngila, P. Ongoma, J. Chacha, Studies of chromium removal from tannery wastewaters by algae biosorbents, *Spirogyra condensata* and *Rhizoclonium hieroglyphicum*, *J. Hazard. Mater.*, 158 (2008) 605–614.
- [21] S. Siddiquee, R. Kobun, S. Al Azad, L. Naher, S. Saallah, P. Chaikaew, Heavy metal contaminants removal from wastewater using the potential filamentous fungi biomass: a review, *J. Microbiol. Biochem. Technol.*, 7 (2015) 384–393.
- [22] P.A. Terry, Characterization of Cr ion exchange with hydrotalcite, *Chemosphere*, 57 (2004) 541–546.
- [23] L. Mercier, C. Detellier, Preparation, characterization, and applications as heavy metals sorbents of covalently grafted thiol functionalities on the interlamellar surface of montmorillonite, *Environ. Sci. Technol.*, 29 (1995) 1318–1323.
- [24] O. Abollino, M. Aceto, M. Malandrino, C. Sarzanini, E. Mentasti, Adsorption of heavy metals on Na-montmorillonite. Effect of pH and organic substances, *Water Res.*, 37 (2003) 1619–1627.
- [25] D. Wu, Y. Sui, S. He, X. Wang, C. Li, H. Kong, Removal of trivalent chromium from aqueous solution by zeolite synthesized from coal fly ash, *J. Hazard. Mater.*, 155 (2008) 415–423.
- [26] M. Majdan, O. Maryuk, S. Pikus, E. Olszewska, R. Kwiatkowski, H. Skrzypek, Equilibrium, FTIR, scanning electron microscopy and small wide angle X-ray scattering studies of chromates adsorption on modified bentonite, *J. Mol. Struct.*, 740 (2005) 203–211.
- [27] V.J. Inglezakis, M. Stylianou, M. Loizidou, Ion exchange and adsorption equilibrium studies on clinoptilolite, bentonite and vermiculite, *J. Phys. Chem. Solids*, 71 (2010) 279–284.
- [28] M.A. Stylianou, V.J. Inglezakis, M.D. Loizidou, A. Agapiou, G. Itskos, Equilibrium ion exchange studies of Zn²⁺, Cr³⁺, and Mn²⁺ on natural bentonite, *Desal. Water Treat.*, 57 (2016) 27853–27863.
- [29] Z. Li, S. Xu, G. Xiao, L. Qian, Y. Song, Removal of hexavalent chromium from groundwater using sodium alginate dispersed nano zero-valent iron, *J. Environ. Manage.*, 244 (2019) 33–39.
- [30] X. Lv, G. Jiang, X. Xue, D. Wu, T. Sheng, C. Sun, X. Xu, Fe⁰-Fe₃O₄ nanocomposites embedded polyvinyl alcohol/sodium alginate beads for chromium(VI) removal, *J. Hazard. Mater.*, 262 (2013) 748–758.
- [31] J. Wu, X.-B. Wang, R.J. Zeng, Reactivity enhancement of iron sulfide nanoparticles stabilized by sodium alginate: taking Cr(VI) removal as an example, *J. Hazard. Mater.*, 333 (2017) 275–284.
- [32] H. Xu, R.-x. Hao, X.-y. Xu, Y. Ding, A.-h. Lu, Y.-h. Li, Removal of hexavalent chromium by *Aspergillus niger* through reduction and accumulation, *Geomicrobiol. J.*, 38 (2021) 20–28.
- [33] Y. Ding, R.-X. Hao, X.-Y. Xu, A.-h. Lu, H. Xu, Improving immobilization of Pb(II) ions by *Aspergillus niger* cooperated with photoelectron by anatase under visible light irradiation, *Geomicrobiol. J.*, 36 (2019) 591–599.
- [34] V. Gómez, M.P. Callao, Chromium determination and speciation since 2000, *TrAC, Trends Anal. Chem.*, 25 (2006) 1006–1015.
- [35] D. He, M. Zheng, T. Ma, J. Ni, Nitrite interference and elimination in diphenylcarbazide (DPCI) spectrophotometric determination of hexavalent chromium, *Water Sci. Technol.*, 2 (2015) 223–229.
- [36] Z. Liu, M.A. Uddin, Z. Sun, FT-IR and XRD analysis of natural Na-bentonite and Cu(II)-loaded Na-bentonite, *Spectrochim. Acta, Part A*, 79 (2011) 1013–1016.
- [37] A. Mansri, K.I. Benabadi, J. François, Chromium removal using modified poly(4-vinylpyridinium) bentonite salts, *Desalination*, 245 (2009) 95–107.
- [38] M. Barkat, S. Chegrouche, A. Mellah, B. Bensmain, D. Nibou, M. Boufatit, Application of algerian bentonite in the removal of cadmium(II) and chromium(VI) from aqueous solutions, *J. Surf. Eng. Mater. Adv. Technol.*, 4 (2014) 210–226.
- [39] D. Park, Y.-S. Yun, J.M. Park, Use of dead fungal biomass for the detoxification of hexavalent chromium: screening and kinetics, *Process Biochem.*, 40 (2005) 2559–2565.
- [40] U. Thacker, D. Madamwar, Reduction of toxic chromium and partial localization of chromium reductase activity in bacterial isolate DM₁, *World J. Microbiol. Biotechnol.*, 21 (2005) 891–899.
- [41] B. Dhal, H. Thatoi, N. Das, B.D. Pandey, Reduction of hexavalent chromium by *Bacillus* sp. isolated from chromite mine soils and characterization of reduced product, *J. Chem. Technol. Biotechnol.*, 85 (2010) 1471–1479.
- [42] A.M. Gutierrez, J.J.P. Cabriaes, M.M. Vega, Isolation and characterization of hexavalent chromium-reducing rhizospheric bacteria from a wetland, *Int. J. Phytorem.*, 12 (2010) 317–334.
- [43] R.M. Bennett, P.R.F. Cordero, G.S. Bautista, G.R. Dedeles, Reduction of hexavalent chromium using fungi and bacteria isolated from contaminated soil and water samples, *Chem. Ecol.*, 29 (2013) 320–328.
- [44] A.A. Al-Homaidan, H.S. Al-Qahtani, A.A. Al-Ghanayem, F. Ameen, I.B.M. Ibraheem, Potential use of green algae as a biosorbent for hexavalent chromium removal from aqueous solutions, *Saudi J. Biol. Sci.*, 25 (2018) 1733–1738.
- [45] M.G. da Fonseca, M.M. de Oliveira, L.N.H. Arakaki, Removal of cadmium, zinc, manganese and chromium cations from aqueous solution by a clay mineral, *J. Hazard. Mater.*, 37 (2006) 288–292.
- [46] M. Faatz, F. Gröhn, G. Wegner, Amorphous calcium carbonate: synthesis and potential intermediate in biomineralization, *Adv. Mater.*, 16 (2004) 996–1000.

- [47] J. Miot, L. Remusat, E. Duprat, A. Gonzalez, S. Pont, M. Poinso, Fe biomineralization mirrors individual metabolic activity in a nitrate-dependent Fe(II)-oxidizer, *Front. Microbiol.*, 6 (2015) 879, doi: 10.3389/fmicb.2015.00879.
- [48] R.L. Kimber, H. Bagshaw, K. Smith, D.M. Buchanan, V.S. Coker, J.S. Cavet, J.R. Lloyd, Biomineralization of Cu₂S nanoparticles by *Geobacter sulfurreducens*, *Appl. Environ. Microbiol.*, 86 (2020), doi: 10.1128/AEM.00967-20.
- [49] A.P. Das, S. Singh, Occupational health assessment of chromite toxicity among Indian miners, *Indian J. Occup. Environ. Med.*, 15 (2011) 6–13.
- [50] E.A. Ashour, M.A. Tony, Eco-friendly removal of hexavalent chromium from aqueous solution using natural clay mineral: activation and modification effects, *SN Appl. Sci.*, 2 (2020) 2042, doi: 10.1007/s42452-020-03873-x.
- [51] M.K. Guria, A.K. Guha, M. Bhattacharyya, A green chemical approach for biotransformation of Cr(VI) to Cr(III), utilizing *Fusarium* sp. MMT1 and consequent structural alteration of cell morphology, *J. Environ. Chem. Eng.*, 2 (2014) 424–433.
- [52] L. Shi, J. Xue, B. Liu, P. Dong, Z. Wen, Z. Shen, Y. Chen, Hydrogen ions and organic acids secreted by ectomycorrhizal fungi, *Pisolithus* sp1, are involved in the efficient removal of hexavalent chromium from waste water, *Ecotoxicol. Environ. Saf.*, 161 (2018) 430–436.
- [53] A.L. Neal, K. Lowe, T.L. Daulton, J. Jones-Meehan, B.J. Little, Oxidation state of chromium associated with cell surfaces of *Shewanella oneidensis* during chromate reduction, *Appl. Surf. Sci.*, 2 (2002) 150–159.
- [54] M. Önal, Swelling and cation-exchange capacity relationship for the samples obtained from a bentonite by acid activations and heat treatments, *Appl. Clay Sci.*, 37 (2007) 74–80.
- [55] M. Holmboe, S. Wold, M. Jonsson, Porosity investigation of compacted bentonite using XRD profile modeling, *J. Contam. Hydrol.*, 128 (2012) 19–32.
- [56] A. Gupta, S.G. Bhagwat, J.K. Sainis, *Synechococcus elongatus* PCC 7942 is more tolerant to chromate as compared to *Synechocystis* sp. PCC 6803, *Biometals*, 26 (2013) 309–319.
- [57] Y. He, L. Dong, S. Zhou, Y. Jia, R. Gu, Q. Bai, J. Gao, Y. Li, H. Xiao, Chromium resistance characteristics of Cr(VI) resistance genes *ChrA* and *ChrB* in *Serratia* sp. S2, *Ecotoxicol. Environ. Saf.*, 57 (2018) 417–423.